NIOSH

National Institute for Occupational Safety and Health

Robert A. Taft Laboratories
Cincinnati OH 45226

EPA

United States Environmental Protection Agency

Office of Environmental Processes and Effects Research
Washington DC 20460

EPA-600/7-81-145
August 1981

Research and Development

Collection Efficiency of Field Sampling Cassettes

Interagency Energy/Environment R&D Program Report

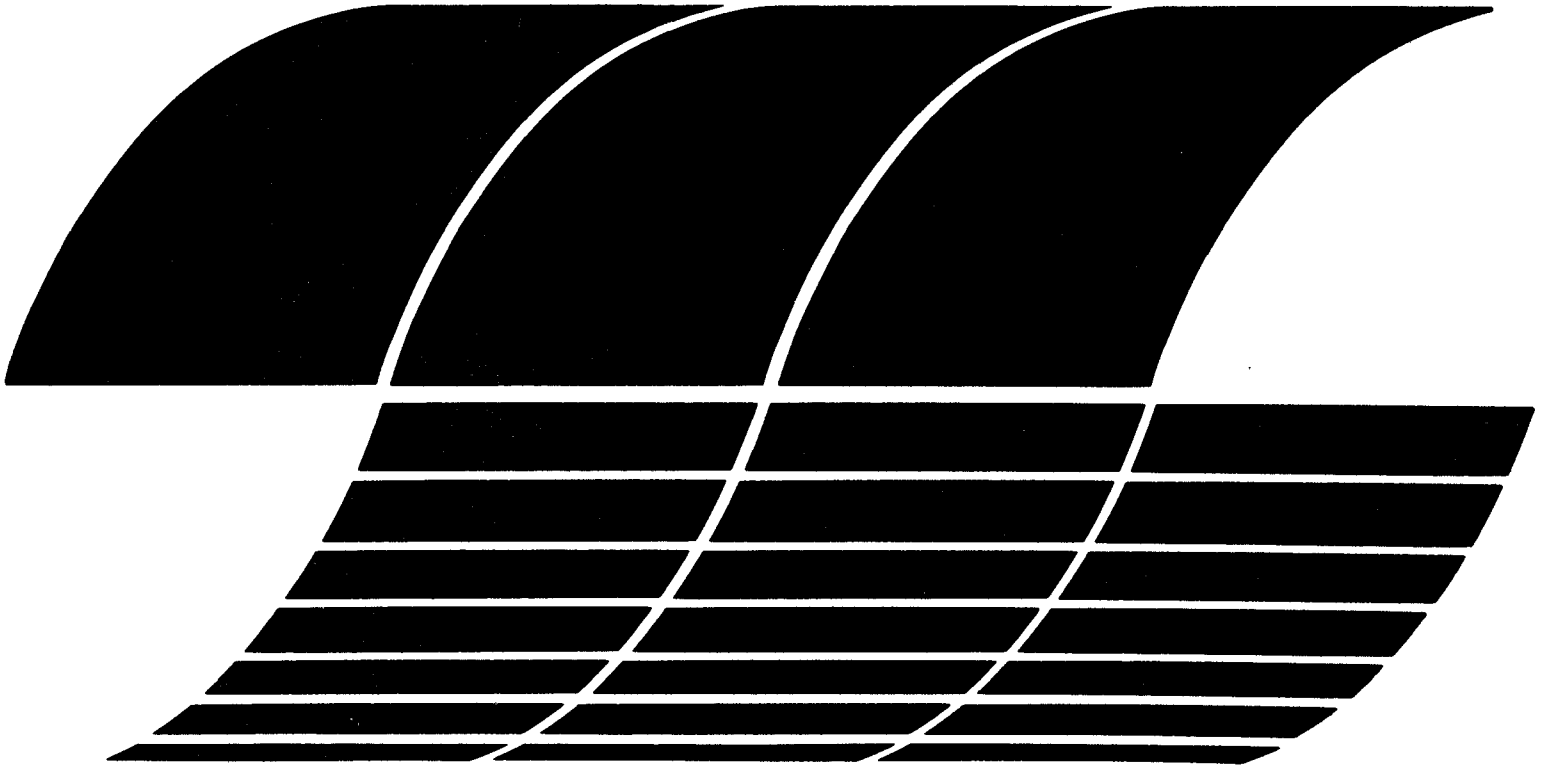

LA-8640-MS

Collection Efficiency of Field Sampling Cassettes

University of California

LOS ALAMOS SCIENTIFIC LABORATORY
Post Office Box 1663 Los Alamos, New Mexico 87545

This report was not edited by the Technical Information staff.

This work was supported by the National Institute for Occupational Safety and Health.

LA-8640-MS

UC-41
Issued: December 1980

Collection Efficiency of Field Sampling Cassettes

C. I. Fairchild
M. I. Tillery
J. P. Smith*
F. O. Valdez

*National Institute for Occupational Safety and Health, Cincinnati, OH 45226.

COLLECTION EFFICIENCY OF FIELD SAMPLING CASSETTES

by

C. I. Fairchild, M. I. Tillery, J. P. Smith, and F. O. Valdez

ABSTRACT

Industrial hygiene particulate samples are often collected under anisokinetic sampling conditions and in crosswinds. Experiments were conducted to quantitate errors associated with sampling under these nonideal conditions.

Three types of field sampling cassettes were tested to determine particle sampling efficiencies for 0, 2, and 5 m/s winds at incidence angles of 0, 90 and 180°. Sampling at one-half or full standard flow rate, 37-mm-diam filters in both open-face and closed-face cassette configurations and a 13-mm polyethylene filter cassette were challenged by monodisperse particles of 4-, 8-, and 21-μm nominal aerodynamic diameter (D_{ae}). Challenge aerosols of Eosin-Y fluorescent dye were generated by a Berglund-Liu vibrating orifice generator, and monodisperse pollen aerosols were generated by nebulization from a water suspension.

Tests were conducted in a chamber in which the cassettes or filter holders were moved to generate a relative wind. Eight filter cassettes mounted symmetrically on a horizontal arm which rotated about a vertical shaft at 250 rpm were positioned so that four cassettes moved at 2 m/s and four at 5 m/s. In addition to two each of the test cassettes, two in-line filter cassettes equipped with isokinetic probes were mounted on the arm. Mass, or number of particles, collected by test cassettes and isokinetic samplers was compared to that collected by stationary filters placed near the rotating arm. Results from tests in the rotating arm chamber were checked against similar tests made in a turbulent flow wind tunnel.

Sampling efficiencies were compared to theoretical values calculated from Belyaev and Levin's theory, and Davies' modification for calm air sampling.

Satisfactory agreement was obtained for 5-μm D_{ae} particles; however, considerable discrepancy was noted with larger particles. The results indicate that corrections must be made to determine concentration when particles collected under nonideal sampling conditions are larger than ~5-μm D_{ae}. Worst case conditions were:

- **The 37-mm open-face cassette oversampled by factors of 2 or more when facing into a wind.**
- **All cassettes undersampled when the relative wind was at large angles to the cassette's inlets.**

INTRODUCTION

Collection of aerosols by filtration for analysis of concentration, composition, and size distribution is used widely in health hazard analysis and air pollution studies. It is usually assumed that the high efficiency filters collect representative samples of the environment. This is particularly true if the sampling is from a still atmosphere. However, unless a sampling system is carefully designed, it is possible that the sample obtained is not representative.

Probably the most important component of a sampling train is the inlet. The inlet may be some type of probe, isokinetic or not, with transfer lines leading to an in-line filter; or the inlet may be an integral part of the filter holder. Numerous types of filter holders are available commercially and large quantities of molded plastic, disposable filter cassettes are used in field sampling because of their convenience and low cost. The cassettes have a variety of inlets and are usually designed for multipurpose sampling.

This study concentrated on three filter cassettes that are used extensively in industrial hygiene field sampling. These cassettes were an in-line (IL) type, 37-mm-diam filter holder, an open-face (OF) type, 37-mm-diam filter holder, and an IL type, 13-mm-diam filter holder. These cassettes are shown in Fig. 1 along with two probes designed specifically to fit a 37-mm in-line cassette and sample isokinetically at 2 and 5 m/s airstream velocity. Little is known of the collection efficiency of these holders (cassettes) in sampling situations such as sampling into a wind, crossflow, or facing 180° to the wind. Also, the flow rate recommended for use with these cassettes is usually set according to the amount of sample required for analysis with little consideration of sampling problems.

THEORY

Three sources of error in sampling particles from airstreams are: (1) particles that deposit on the walls of the sampler inlet may be a significant fraction of the particles entering, (2) particles that rebound from the frontal lip of the sampler inlet may enter the sampler, producing an oversampling of particles; and (3) a disproportionate number of large particles enter or pass the sampler inlet because the particles cannot follow the fluid streamlines.

The source of error due to wall deposition is generally not amenable to theoretical analysis. Some work, notably Sehmel's,[1] has been reported wherein deposition in long ducts has been treated theoretically; however, no good predictive equations are available for complex inlet geometries. The amount of particulate material depositing on internal surfaces is dependent upon

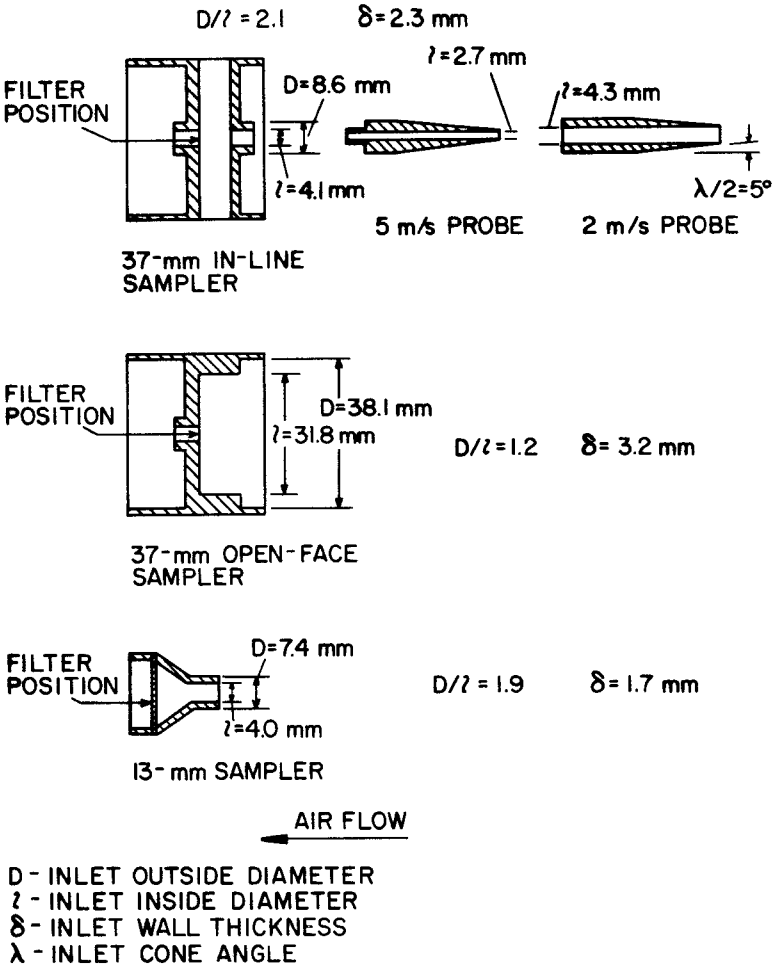

Fig. 1.
Cross sections of sampling cassettes and isokinetic probes.

particle inertia and a number of factors specific to the aerosol and sampling system. These factors include aerosol material, sampler material, relative humidity, wall roughness, and inlet channel geometry (bends, expansions, etc.). In practice, either the deposition losses of a sampling system are determined in preliminary experiments, or else deposited particles are cleaned from internal surfaces after each sampling period and included in the analysis.

Rebound of particles from the sampler inlet lip generally contributes little error to the measurement of aerosol mass concentration, but it may bias a size distribution measurement significantly because only the large particles strike and rebound. Rebound particles tend to be carried into the sampler under superisokinetic conditions, whereas, in subisokinetic sampling they are primarily carried away from the inlet (Fig. 2). Some rebound error may occur even at isokinetic sampling conditions with thick wall inlets because of turbulence at the inlet.

The largest sampling errors are produced by anisokinetic sampling or sampling at an angle to the airstream. These errors, caused by particle inertia, result in a failure of particles to follow the airflow. Primary parameters defining whether particles are captured by the inlet airflow are particle size, airstream velocity, sampler inlet air velocity, sampler inlet dimensions, and angle of the inlet to the airstream. Particle size is defined better as particle inertia in the airstream according to the Stokes number:

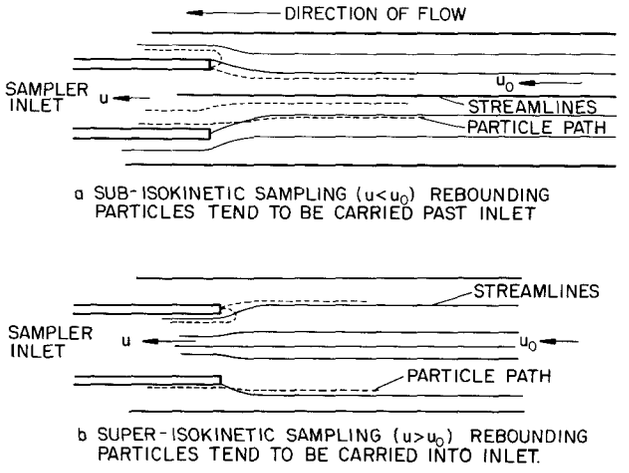

Fig 2.
Conditions prevailing for sub- and super-isokinetic sampling.

$$STK = (v_s \cdot u_o)/(l \cdot g) \quad , \tag{1}$$

where v_s is the particle settling velocity, u_o the airstream velocity, g the acceleration of gravity, and l a characteristic linear dimension of the system, in this case the sampler inlet inside diameter. The ratio of the sampler flow velocity and airstream velocity is the isokinetic parameter, u/u_o, which defines flow conditions at the sampler inlet.

Belyaev and Levin[2] found in analyzing sampling errors that samplers must also be divided into "thick-wall" and "thin-wall" types. If the outer diameter is D, δ the wall thickness, and λ the included angle of taper of the wall from the inlet, then the sampler is thin-walled at any value of STK and λ, if $\delta/l \leq 0.05$ (D/l is ≤ 1.1). According to Belyaev and Levin's experiments, a fractional sampling efficiency of 1 cannot be achieved with thick-wall samplers in moving airstreams. Cassettes tested in this study were not of a simple tubular design (Fig. 1), and according to the criteria of Belyaev and Levin all of the samplers have thick-walled inlets, that is, for all three cassettes $D/l > 1.1$ and in addition $\delta/l > 0.05$.

The sampling efficiency of the cassettes tested is defined as the fractional ratio of the measured to the true aerosol concentration,

$$E = c/c_o \quad , \tag{2}$$

where E is fractional efficiency, c the aerosol concentration determined from the mass collected on the cassette filter, and c_o the true or reference aerosol concentration determined independently by a method known to yield true concentration. The efficiency is defined by Belyaev and Levin[2] as an aspiration coefficient

$$A = c/c_o \quad . \tag{3}$$

The aspiration coefficient can be further represented by

$$A = A_i\, A_d\, A_y \quad , \tag{4}$$

where A_i is the component of the aspiration coefficient characterizing concentration changes due to aerodynamic and inertial forces (represented by STK and u/u_o), A_d, the component characterizing the concentration decrease in the sampler due to wall deposition, and A_y the component characterizing particle rebound. A_y and A_d can only be determined by experiment, consequently in Belyev and Levins' theoretical analysis, only A_i is considered:

$$A_i = c/c_o \quad . \tag{5}$$

In a subsequent study of sampling inlets Belyev and Levin[3] proposed a semiempirical relationship for the inertial efficiency coefficient. This coefficient, A_i, based upon their experiments as well as those of Badzioch,[4] and Voloschuk and Levin,[5] related the efficiency of thin-wall samplers to STK and u/u_o:

$$A_i = 1 + [(u_o/u) - 1]\, \beta\, (STK, u/u_o) \quad , \tag{6}$$

where u_o/u is the inverse of the isokinetic parameter, and β was found experimentally to be a function of both STK and u/u_o,

$$\beta(STK, u/u_o) = 1 - \{1/[1 + (2 + 0.62\, u/u_o)STK]\} \quad . \tag{7}$$

Substituting the expression for β, the final equation for A_i is

$$A_i = 1 + (u_o/u - 1)\, /1 - \{1/[1 + (2 + 0.62\, u/u_o)STK]\}/ \quad . \tag{8}$$

Strictly speaking, Eq. (8) applies only to thin-wall inlets in significant winds and at zero incidence angle ($\alpha = 0°$).

The calculated theoretical coefficient for calm wind, A_o, must be defined differently because at $u_o = 0$ Eq. (8) goes to $A_i = 0$ for all sampling conditions. Davies[6] recommends another relation for $u_o \rightarrow o$ using Stokes number, K_u, based on flow within the sampling nozzle rather than STK based on the airstream. Then as u_o approaches zero, A_i approaches A_o:

$$A_o = 1 - \{0.62\ K_u/[0.05\ K_u + (1 + 0.62\ K_u]\} \quad (9)$$

A_o is independent of u_o and depends only on K_u in no wind conditions.

The other sampling condition which causes significant error, sampling at an angle α to the wind (α = angle in degrees between wind direction and sampler inlet axis), had been studied little until recently. Durham and Lundgren[7] introduced empirical equations based upon their experiments as well as those of Belyaev and Levin. These equations predict that the sampling efficiency decreases rapidly as α goes to 90°, becoming essentially 0 at 90°. Raynor[8] found similar experimental results for α up to 90° but also found the efficiency to increase slightly as α continued to increase from 90 to 120°. He found for an open-face, thick-wall sampler (3.2-cm o.d. by 1.9-cm i.d.) the minimum efficiency against 6-μm particles was near zero at α = 90° but increased to approximately 50% at α = 120°. However, Raynor did not correct for wall deposition in the sampler. Rajendran,[9] using models based upon the Navier Stokes equations of fluid motion and equations of particle dynamics obtained numerical solutions which showed, in agreement with Durham, that the collection efficiency of samples decreases to very low values at angles of incidence (α) approaching 90°.

EXPERIMENTAL

The experimental plan for this investigation called for examining the performance of the three cassettes against three aerosol particle sizes, three airstream velocities, and three airstream incidence angles using two sampling flow rates. One flow rate, designated the standard flow rate, was an average of the rates recommended by the National Institute for Occupational Safety and Health (NIOSH) in present sampling practice. The other flow rate was one-half of this standard and was used to simulate an extreme condition of poorly calibrated flowmeter, or an overloaded, high pressure drop filter. Sampling flow rates ranging from 1 to 5 L/min for 37-mm filter holders, and 0.1 to 1 L/min for 13-mm filter holders are used in present field sampling practice. For this investigation representative average sampling flow rates of 1.8 L/min and 0.5 L/min for the 37- and 13-mm cassettes respectively were chosen as standard flow rates. Three replicates of each condition were planned (Table I), although for calm wind sampling conditions either two or four samples were obtained because of test equipment limitations. Thus a total of 396 samples for three test cassettes, and 300 reference samples collected by four reference samplers were required. In addition to these filter samples, it was planned to analyze about 25% of the cassettes for particle deposition on the inlet wall. An additional 32 samples were obtained in a separate wind tunnel.

The number of samples and analyses required in the allotted time introduced a problem concerning equipment. As described in a review by Fuchs,[10] experiments to determine sampling efficiency against controlled winds have usually been performed in wind tunnels. In the present investigation, where a minimum of three cassettes plus a reference sampler were to be tested in identical conditions, a tunnel diameter of 20 cm was required to prevent interference effects between the four samplers. At a wind velocity of 5 m/s a volume of 10 000 L/min (340 cfm) of aerosol was required. Then to limit each test run to 2 h assuming 25 μg of mass is required on each filter for reasonable analytical accuracy (fluorometric analysis precision of ± 2 μg) an aerosol concentration of approximately 0.4 μg/L for the 500 cc/min sampling rate of the 13-mm filter cassette was required. To produce this concentration an aerosol generation rate of 4 mg/min was required. This is an excessive generation rate for monodisperse particles >1-μm diam. Another approach

TABLE I

EXPERIMENTAL PLAN

Rotating Arm Chamber

Angle of Incidence α (°)	Sampling Flow Rate	Nominal Particle Diameter, D_{ae} 4 μm, Airstream Velocity, u_o (m/s) 0	2	5	8 μm 0	2	5	21 μm 0	2	5
0	Std[a]	4[b]	3	3	4	3	3	4	3	3
	1/2 Std	4	3	3	4	3	3	4	3	3
90	Std	---	3	3	---	3	3	---	3	3
	1/2 Std	---	---	---	---	3	3	---	---	---
180	Std	---	3	3	---	3	3	---	3	3
	1/2 Std	---	---	---	---	3	3	---	---	---

Wind Tunnel

0	Std			4			4			4
180	Std						4			

Total number of test samples in RAC: 372
Total number of reference samples in RAC: 60 isokinetic + 240 stationary: 300
Total number of wind tunnel samples: 16 test sampler + 16 isokinetic: 32
Total number of cassettes analyzed for wall losses: ~200

[a]Std flow was 1.8 L/min for 37-mm cassettes and 0.5 L/min for 13-mm cassettes.
[b]Numbers in table indicate number of replicates for each condition.

considered was to employ a closed cycle (recirculating) wind tunnel to permit increasing the concentration to an equilibrium value. Disadvantages of this technique are (1) particle loss on wall and air mover, particularly for large particles, (2) length of time to build to equilibrium concentration, and (3) possible heat and moisture removal problems.

An alternative to moving the aerosol past the samplers is to move the samplers through the aerosol to achieve a desired relative wind velocity. If the motion of the samplers is confined to a relatively small volume then the requirements for aerosol generation rate are correspondingly decreased. This type sampling chamber was constructed for this investigation using a cylindrical chamber (barrel) with the samplers mounted on a vertical shaft and crossarm so as to move in a horizontal circle around the shaft. In addition to decreasing the demands on the aerosol generation system, the moving sampler system had other advantages. The system was more compact than a wind tunnel, several samplers could be tested simultaneously, and the turbulence generated within a relatively large diameter chamber simulates the scale and intensity of turbulence found in normal industrial sampling environments better than does a small diameter wind tunnel.

The primary disadvantage to moving the samplers rather than the air arises from the necessity of proving the two methods equivalent. It was found to be impractical to measure the relative wind velocity directly in front of each sampler with sensors requiring leads, because of twisting or sliding contact electrical noise from the rotational motion, or in the case of remote measurement (laser doppler velocimeter), because of the expense. Consequently, results obtained in the moving

sampler apparatus and results obtained from limited tests in a small conventional wind tunnel were compared to establish the validity of the moving sampler concept.

The primary apparatus used to test the sampling efficiency of the filter holders was a plastic drum with an internal rotating arm. The drum was 0.6-m diam by 0.8-m high with a 3/4-in. thick, removable Plexiglas top, which could be clamped to the drum flange gasket to form an airtight seal. This Plexiglas top served to support an inverted "T" shaped rotatable arm (Fig. 3), which supported up to eight filter cassettes. The inverted "T" arm was rotated about its vertical shaft by a motor-pulley-belt drive above the Plexiglas top. The shaft was supported by ball bearing bushings and a rotating seal, which prevented air leakage to or from the drum. The inverted "T" arm, or rotating arm, was made of hard drawn copper tubing which had four tubular, threaded filter holder mounts for two filter cassettes silver soldered symmetrically to the arm at 7.5 and 20 cm from the center of the horizontal cross tube (Fig. 4). Thus, a total of eight cassettes could be mounted on the rotating arm facing any horizontal direction, four at 7.5 cm and four at 20 cm from the center of rotation. A calibrated critical flow orifice was positioned behind each filter cassette. At the top of the vertical shaft another rotating seal connector (not visible in Fig. 3) joined the shaft to a flexible vacuum hose leading to a pump. The pump maintained a vacuum of <150 torr absolute on the tubular rotating arm manifold so that all eight orifices operated in the critical flow pressure range. Above and below the rotating arm two similar fixed arms held two filter holders each to serve as stationary reference samplers. The stationary arms were positioned as close to the rotational plane of the samplers as possible. The stationary samplers, which sampled at 5 L/min, were also controlled by critical flow orifices. Two additional tubes, an aerosol inlet and an exhaust tube, extended through the drum sidewall to near the drum center. The upper tube near the chamber top had a baffle on the intake and two parallel filters on the exhaust end external to the chamber. The lower tube, near the chamber bottom, served to introduce aerosols into the chamber. A circular baffle plate immediately above the aerosol inlet prevented aerosol

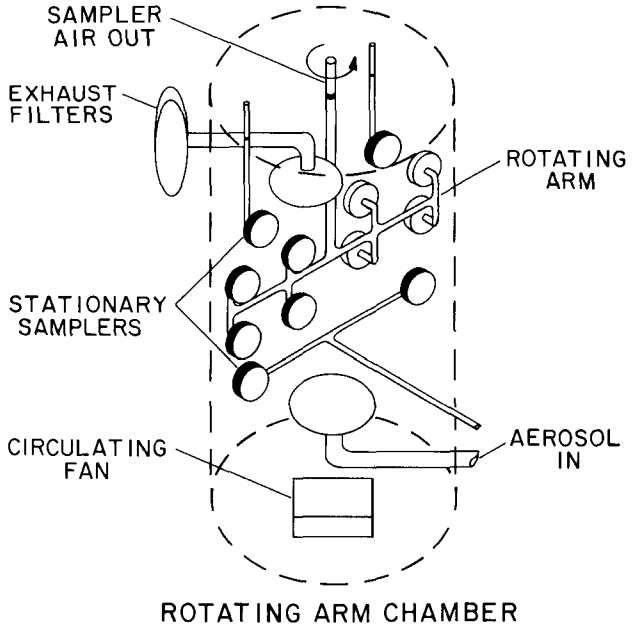

Fig. 3.
Rotating arm chamber (RAC) test apparatus.

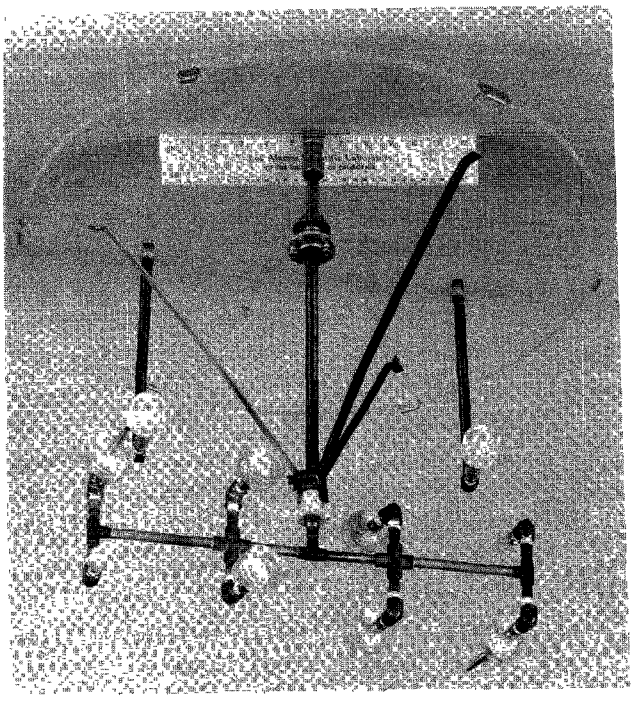

Fig. 4.
Rotating sampler arm.

from jetting up into the chamber. At the bottom of the chamber a 100-cfm fan provided a circulating, mixing airflow to produce a uniform concentration of aerosol within the chamber. Additional tubular probes were inserted through the side wall of the chamber to withdraw samples for particle sizing.

A small wind tunnel (WT) was also used to duplicate some tests made in the rotating arm chamber (RAC). This tunnel was 8-cm diam by 2-m long and had a high-efficiency particulate air (HEPA) filter on the inlet and exit (Fig. 5). Aerosol was introduced through a side arm near the tunnel inlet into the center of the tunnel and a Stairmand disk immediately downstream of the aerosol inlet promoted mixing with the inlet dilution air. The length to diameter ratio of the tunnel insured that well developed turbulent flow existed at the test section. Only two test samplers were accommodated in the WT, one in-line type 37-mm holder with an isokinetic inlet and one without an isokinetic inlet. These were tested at only one velocity (5 m/s), two particle sizes (4- and 8-μm D_{ae}), and two sampler orientations (0 and 180°). The test cassette was placed alternately in the upstream and downstream positions of the mounting fixture (Fig. 5).

Monodisperse particles <20-μm D_{ae} were generated from isopropyl alcohol solutions of Eosin-Y fluorescent dye. A Berglund-Liu vibrating orifice generator with a pneumatic system to feed dye at a constant rate produced spherical particles with geometric standard deviations (σ_g) from 1.04 to 1.10. The dye particle sizes were measured primarily by photomicrographic techniques. Samples were obtained from the test chambers on Nucleopore filters, imaged and photographed in a scanning electron microscope, and sized with a Zeiss TGZ-3 comparator. A Royco 220 light photometer, calibrated against Eosin-Y particles, gave supplementary size information for particles <5-μm diam.

Inlet efficiency tests were generally of about 30-min duration when made in the RAC and about 3 h when made in the WT. Prior to starting each test, particle size generated from the Berglund-Liu apparatus was adjusted while dumping the aerosol through an exhaust filter. After the aerosol was stabilized and introduced into the RAC, a period of 5 min was allowed for concentration to reach equilibrium before the sampler arm rotation was initiated and sampling started.

During the test the rotational speed of the sampler arm was determined with a "Strobotac", light photometer measurements were made, and a Nucleopore filter sample was taken. After test completion, filters were removed from the cassettes and placed in labeled Petri dishes. Each filter was washed with 200 ml of twice distilled water, then an aliquot was analyzed in a Turner fluorometer. From the fluorescence measurement, wash volume and dilution factor the mass of particles on the filter could be calculated. Wash tests indicated that the filters retained 3.0 ± 0.5% of the original Eosin-Y dye after washing with 200 ml water. Since this was true of both the test and reference filters, no correction was made for this loss.

Particles >20 μm used in these tests, short ragweed and giant ragweed pollen, were nebulized from a water suspension in a manner similar to that used by Lautner and Fisher.[11] Due to the large aerodynamic size of these particles a large fraction redeposited within the nebulizer or the

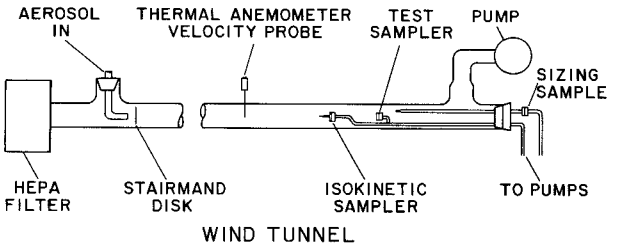

Fig. 5.
Wind tunnel (WT) test apparatus.

short transfer line to the test chamber. This produced a very low concentration (<1 particle/cc) of pollen particles within the test chamber. Rather than sample long enough to obtain sufficient mass for weighing, the test filters containing pollen particles were counted using a Zeiss microscope at 60× with low angle side lighting. Initially, the entire filter area was searched; however, it was found that the counts from four traverses across the diameter in different directions, multiplied by an area factor, provided total counts within 15% of counts obtained by scanning the entire filter.

Sizing pollen particles was performed with the same Zeiss microscope using a Porton graticule in one eyepiece at a magnification of 160×. Short ragweed pollen was found to be 20.3-μm diam with σ_g <1.05 and giant ragweed pollen was 24.2 μm with σ_g = 1.04. Aerodynamic diameters were obtained independently from a falling particle-flash photography apparatus. A stroboscopic light provided periodic illumination of pollen falling within a glass column of clean, still air. Time-exposure photographs of the particles were not used unless a minimum of three images were equidistant vertically from one another. Aerodynamic diameters calculated from the images were 21.2 ± 2.7 μm and 25.3 ± 1.9 μm for short ragweed and giant ragweed spores respectively. The particle densities (assuming perfect spheres) of 1.08 and 1.09 calculated from the measured physical and aerodynamic diameters were corroborated qualitatively by the observation that the particles settled to the bottom of a water suspension over a period of 24 h. Considering the precision of the aerodynamic diameter measurements, nominal diameters of 21 and 25 μm were used for all calculations.

RESULTS

$\alpha \approx 0°$

Results from cassette inlet tests for $\alpha = 0°$ are compiled in Tables II and III. Table II, containing results for calm wind ($u_o = 0$), is discussed separately because Davies' method of calculation is used to calculate A_o in the interval $0.06 < u_o/u < 1$ and $0.05 \leq K_u < 6.3$ (recommended by Davies). Some K_u and u/u_o values are below the recommended K_u range, but because Eq. (5) approaches 1 as K_u decreases, the values in Table II should be valid. Table III contains results from all tests at $u_o > 0$ and zero angle of incidence for both one-half and full standard sampling flow rates. Individual sample values have been averaged into groups of three or more samples (occasionally only two samples were available/group) which have closely matched parameters (u/u_o, STK). Most of the columns tabulated are dimensionless; only the airstream velocity, u_o, and aerodynamic diameter, D_{ae}, have dimensions. The experimental values of concentration measured by each filter sampler divided by true concentration (measured by stationary sampler), c/c_o, are compared to A_i (or A_o) in the final column of the tables. Thus the final column indicates the ratio of the experimental results to the theoretical value. A_i is the theoretical sampling efficiency only for inertial effects and accounts neither for particles deposited on the cassette walls nor for particles rebounding from the wall (lip) of the cassette. For this reason wall losses were determined independently, and c/c_o in all tables has been adjusted for cassette wall loss, but not for rebound loss (or gain).

The tabulated values of c/c_o and $c/c_o/A_i$ from Tables II and III are plotted in Figs. 6 and 7. Data from Table II for $u_o = 0$ are shown as c/c_o vs D_{ae} in Fig. 6 because the large range of K_u (10^{-5} to 3.7) makes an abscissa scaled to D_{ae} preferable. The results from Table III for $u_o > 0$, including full and one-half standard sampling flow, are shown as c/c_o vs STK (Fig. 7). Several of the data from the tables have been combined in Figs. 6 and 7 to avoid the confusion of multiple points and overlapping error bars at the same D_{ae} or STK. Data from the isokinetic (IK) samplers are not plotted in Fig. 7 but are included in later graphs.

TABLE II

SAMPLING RESULTS FOR $U_0 = 0$

Sampling Conditions and Cassettes	u (m/s)	D_{ae} μm	K_u [a]	c/c_o [b]	A_o [c]	$c/c_o/A_o$
STANDARD FLOW RATE						
1L[d]	2.4	2.3	0.01	(8) 1.05 ± 0.05 (5)	0.99	1.06
		7.8	0.11	(6) 1.11 ± 0.10 (9)	0.94	1.18
		25	1.13	(4) 1.6 ± 0.81 (51)	0.60	2.7
OF	0.04	2.3	2.2×10^{-5}	(12) 1.10 ± 0.09 (8)	1.00	1.10
		7.8	2.3×10^{-4}	(6) 1.19 ± 0.04 (4)	1.00	1.19
		25	2.0×10^{-3}	(4) 1.3 ± 0.21 (5)	1.00	1.3
13-mm IL	0.7	2.3	3.0×10^{-3}	(8) 1.01 ± 0.19 (19)	1.00	1.01
		7.8	0.03	(6) 0.68 ± 0.19 (28)	0.98	0.69
		25.0	0.33	(4) 0.84 ± 0.49 (58)	0.83	1.01
1/2 STANDARD FLOW RATE						
1L	1.2	6.2	0.07	(4) 0.93 ± 0.08 (9)	0.96	0.97
		7.8	0.11	(8) 0.78 ± 0.27 (35)	0.94	0.83
OF	0.02	6.2	1.5×10^{-4}	(4) 1.43 ± 0.12 (9)	1.00	1.43
		7.9	2.4×10^{-4}	(8) 1.20 ± 0.28 (24)	1.00	1.20
13-mm IL	0.3	7.4	0.03	(12) 0.51 ± 0.10 (20)	0.98	0.52

[a] For $u_0 = 0$, K_u is based on u for each cassette.
[b] c/c_0 is in the format: (No. of samples) mean ± std dev (COV).
[c] A_0 is calculated from Eq. (5).
[d] Cassettes are: IK, 37-mm ISOKINETIC; IL, 37-mm IN-LINE; OF, 37-mm OPEN-FACE; 13-mm IL, 13-mm IN-LINE.

For calm air sampling ($u_o = 0$), Table II and Fig. 6 show that both the 37-mm IL and OF cassettes oversample increasingly for increasing D_{ae}. This is contrary to Davies' sampling theory for calm conditions. The error bars at $D_{ae} = 25$ μm suggest that experimental precision may account for the contradiction; however, other conditions such as nonzero airstream velocities present at the test or reference samplers could affect the results. In contrast to the 37-mm cassettes, the 13-mm IL cassettes exhibited good agreement with expected collection efficiency, A_o, even though the precision of the data is poor.

Sampling into a wind (Table III and Fig. 7) produced data consistent with Belyaev and Levin's theory [Eq. (4)] in that all samplers exhibited increasing oversampling with increasing STK for $u/u_o < 1$. The oversampling is pronounced even at STK < 0.1 for the OF cassette because of the low u/u_o ratio observed for this configuration.

To compare the test results obtained at $\alpha = 0°$ against the sampling theories outlined previously the collection efficiency, c/c_o, was normalized to the A_i (or A_o) value by dividing by A_i (or A_o). This normalized value, $c/c_o/A_i$, is listed in the final column of Tables II and III. If the experimental value (c/c_o) agrees with theory (A_i or A_o) then this final column shows a value near one, as it does for most isokinetic or small particle sampling. The normalized values, $c/c_o/A_i$ from Tables II and III are plotted vs the corresponding A_o or A_i on the abscissa (labeled A_i) in Fig. 8.

TABLE III

SAMPLING RESULTS FOR $\alpha = 0^o$

Sampling Conditions and Cassettes	u_o (m/s)	u/u_o	D_{ae} (μm)	STK	c/c_o [a]	A_i [b]	$c/c_o/A_i$
STANDARD FLOW							
U_o = 5 m/s, α = 0°							
IK [c]	5.1	0.96	4.6	0.2	(6) 0.97 ± 0.23 (24)	1.01	0.96
	5.1	0.95	7.2	0.3	(10) 0.97 ± 0.17 (17)	1.03	0.94
	5.1	0.94	21	2.3	(3) 3.9 ± 1.8 (46)	1.07	3.7
IL	5.1	0.43	4.6	0.06	(5) 1.10 ± 0.08 (7)	1.13	0.97
	5.1	0.45	7.2	0.22	(6) 1.25 ± 0.07 (6)	1.41	0.89
	5.1	0.49	21	1.93	(3) 5.4 ± 0.40 (8)	1.86	2.92
OF	5.1	7×10^{-3}	5.0	0.02	(2) 1.42	4.6	0.31
	5.1	7×10^{-3}	7.5	0.025	(9) 1.40 ± 0.25 (18)	8.0	0.18
	5.1	8×10^{-3}	21	0.27	(2) 12.0	45.0	0.27
13-mm	5.1	0.20	4.5	0.07	(7) 1.29 ± 0.58 (45)	1.65	0.78
	5.1	0.13	7.4	0.23	(5) 1.42 ± 0.86 (61)	3.19	0.45
	5.1	0.15	21	1.93	(3) 7.6 ± 1.7 (23)	5.84	1.3
IL (WT)	5.1	0.50	3.5	0.05	(5) 1.07 ± 0.30 (28)	1.08	1.0
	5.1	0.46	7.4	0.22	(7) 1.08 ± 0.07 (7)	1.35	0.80
U_o = 2 m/s, α = 0°							
IK	1.9	1.04	4.6	0.03	(5) 0.80 ± 0.06 (8)	1.00	0.80
	1.9	1.02	7.4	0.08	(5) 0.93 ± 0.16 (18)	1.00	0.93
	1.9	1.02	21	0.60	(3) 2.23 ± 0.40 (18)	0.99	2.3
IL	1.9	1.25	5.9	0.06	(3) 1.03 ± 0.05 (5)	0.98	1.07
	1.9	1.28	7.6	0.09	(7) 1.01 ± 0.25 (25)	0.96	1.05
	1.9	1.36	21	0.71	(3) 5.7 ± 1.21 (21)	0.82	7.0
OF	1.9	0.02	4.6	5×10^{-3}	(5) 0.94 ± 0.07 (8)	1.22	0.77
	1.9	0.02	7.4	0.01	(5) 1.15 ± 0.28 (25)	2.04	0.56
	1.9	0.02	21	0.09	(3) 8.1 ± 0.35 (4)	8.6	0.94
13-mm	1.9	0.27	5.9	0.06	(2) 1.68	1.28	1.31
	1.9	0.30	7.9	0.10	(7) 0.93 ± 0.39 (41)	1.40	0.66
	1.9	0.28	22	0.71	(3) 4.3 ± 2.5 (59)	2.4	1.8
1/2 STANDARD FLOW							
IL	1.9	0.63	7.1	.08	(3) 0.82 ± 0.31 (37)	1.09	0.75
	5.2	0.22	7.2	.20	(5) 1.6 ± 0.5 (31)	2.12	0.75
	5.2	0.24	21.0	1.9	(3) 3.2 ± 2.1 (66)	3.6	0.89
OF	1.9	0.01	7.0	0.01	(2) 0.88	2.9	0.30
	5.2	3.7×10^{-3}	7.1	0.03	(3) 0.83 ± 0.10 (12)	14.2	0.06
	1.9	0.01	21.0	0.09	(5) 9.9 ± 6.0 (60)	17.1	0.58
	5.2	3.5×10^{-3}	21	0.24	(2) 10.4	93.6	0.11
13-mm	1.9	0.15	7.1	0.08	(3) 1.11 ± 0.08 (7)	1.9	0.58
	5.2	0.50	7.0	0.20	(3) 1.41 ± 0.23 (16)	6.3	0.23
	1.9	0.12	21.0	0.71	(2) 4.8	5.5	0.09
	5.2	0.06	21.0	1.9	(5) 3.0 ± 0.9 (30)	14.5	0.21

[a] c/c_o is in the format: (No. of samples) mean ± std dev (COV).
[b] Cassettes are: IK, 37-mm ISOKINETIC; IL, 37-mm IN-LINE; OF, 37-mm OPEN-FACE; 13-mm, 13-mm IN-LINE; (WT), tested in wind tunnel.
[c] A_i is calculated from Eq. (5) at u_o = 0.

Again, if c/c_o equaled A_i, the plotted points would lie along a horizontal line at $c/c_o/A_i = 1$ for any A_i. In fact, the $c/c_o/A_i$ values decrease monotonically as A_i increases. Also discernible in Fig. 8 are two distinct groups of data. Examination of the data reveals that the upper group contains only data for particles with $D_{ae} > 20$ μm, whereas the lower group contains data only for $D_{ae} < 12$ μm. Most of the points which do not lie distinctly in one or the other group are from tests at one-half standard sampling rate. Therefore, only points resulting from full standard sampling flow rate tests are shown in Fig. 9. With the exception of 1 or 2 points the groups are distinct and have nearly equal slopes. Regression analysis of the two groups of data provides analytical expressions in the form of power functions. The specific functions found to describe sampler efficiency at α = o° are:

$$c/c_o \cdot A_i^{-1} = 1.1\ A_i^{-0.72} \text{ for } 2\text{-}\mu m \leq D_{ae} \leq 12\ \mu m;\ r = 0.82 \quad , \tag{10}$$

$$\text{or } c/c_o = 1.1\ A_i^{0.28} \quad ,$$

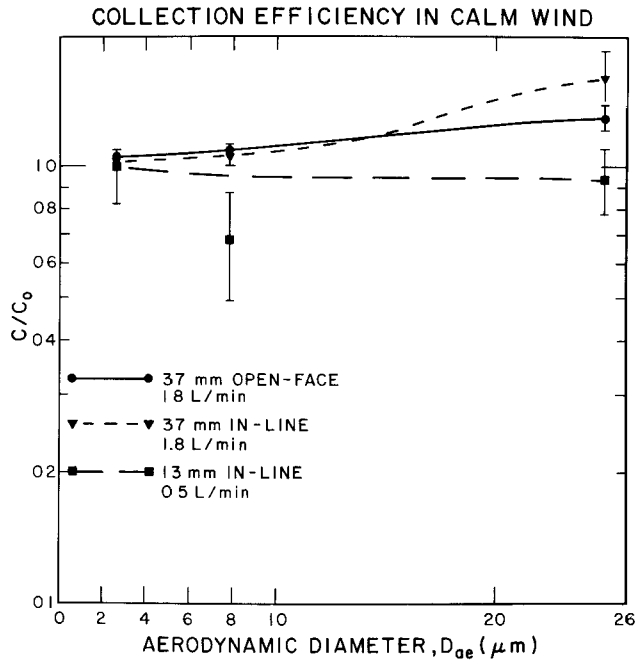

Fig. 6.
Collection efficiency (c/c_o) as a function of aerodynamic diameter in no wind conditions.

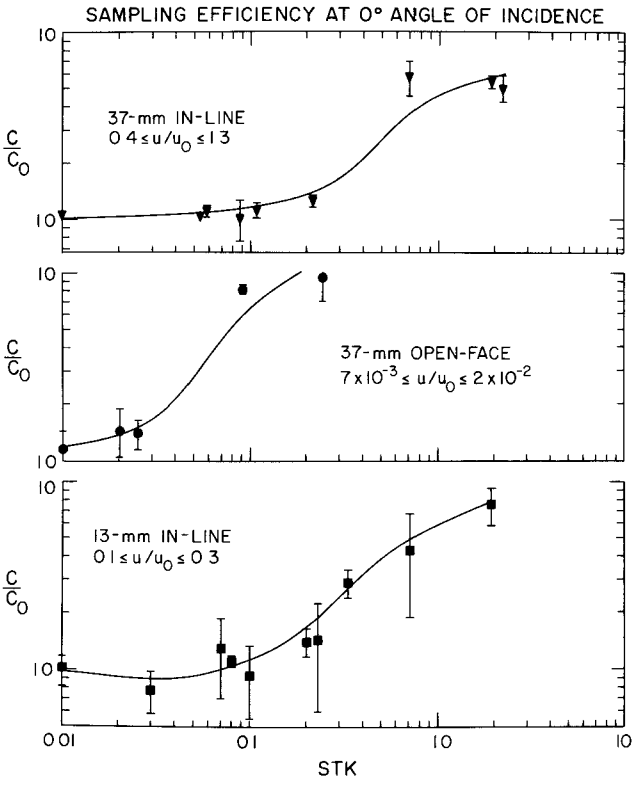

Fig. 7.
Measured collection efficiency (c/c_o) as a function of STK in three wind conditions and two sampling flow rates at $\alpha = 0°$.

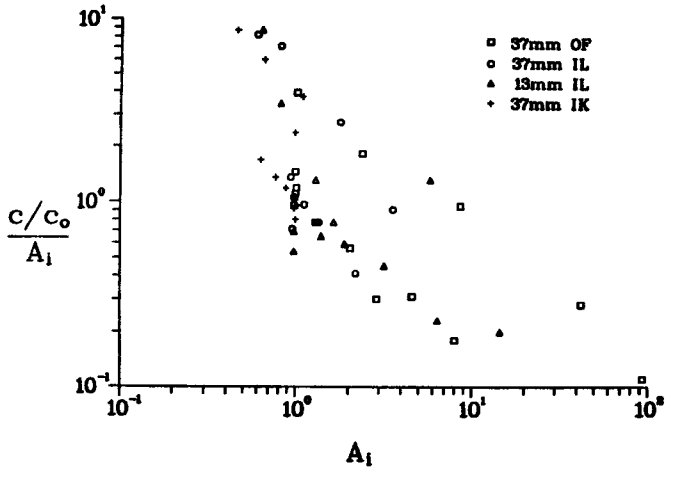

Fig. 8.
Measured collection efficiency (c/c_o) normalized to A_i, plotted as a function of A_i for all sampling conditions at $\alpha = 0°$.

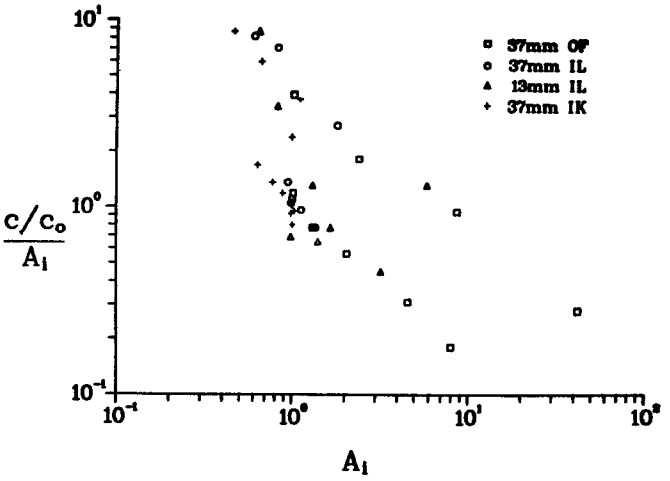

Fig. 9.
Measured collection efficiency (c/c_o) normalized to A_i, plotted as a function of A_i for standard flow rate conditions at $\alpha = 0°$. Regression lines are shown for particles with $D_{ae} > 20\ \mu m$ (upper) and $D_{ae} \leq 12\ \mu m$ (lower).

and

$$c/c_o\ A_i^{-1} = 4.3\ A_i^{-0.74} \text{ for } 21\ \mu m \leq D_{ae} \leq 25\ \mu m;\ r = 0.96\ ,$$

$$\text{or } c/c_o = 4.3\ A_i^{0.26}\ . \tag{11}$$

The two power functions are nearly parallel over the range of calculated A_i and the primary difference in the two groups of data is their displacement from one another. Since $c/c_o/A_i$ is nearly 1 for <12-μm D_{ae} spheres when A_i is 1 (Fig. 9), it appears that these spheres give more valid results than do the larger spheres. At the present time no reason is known for the anomalous behavior of D_{ae} > 20-μm spheres. Nor is the reason for the decrease of $c/c_o/A_i$ with increasing A_i known unless it is due to particle bounce from the thick wall of the inlet. This seems unlikely, however, because the difference between c/c_o and A_i is large to be caused by bounce, and because the isokinetic samplers, which had very thin walls, also exhibit c/c_o much larger than A_i when 21- to 25-μm D_{ae} challenge aerosols are used (Table III). One known error in the measurement of the reference concentration (C_o) of large particles in calm air occurs because a finite volume of air beneath the cassette becomes devoid of particles after a few seconds of sampling. The settling velocity of large particles prevents replenishment of this volume with particles. Calculations indicate however, that this effect decreases C_o by only 9% for 20-μm D_{ae} particles; considerably less than the difference in Eqs. (10) and (11). The most probable explanation for the different results for large or small particles lies in the fact that different techniques were used for small and large particle tests. These include different particle material, generation method, and size measurement method (see experimental section), and in combination could have produced significant differences in results.

Using Eqs. (10) and (11) to calculate the collection efficiency of the cassettes for 5-, 10-, 15-, and 20-μm D_{ae} particles, a set of empirical curves (Fig. 10) was derived to predict the performance of each cassette at $\alpha = 0°$ against winds of 2 and 5 m/s. Because no data were obtained between 12-μm $\geq D_{ae} \leq$ 21 μm, and the equations differ above and below this range, 15-μm D_{ae} was used as the crossover between Eqs. (10) and (11); that is, c/c_o values from each of Eqs. (10) and (11) were averaged to force the equations together at 15-μm D_{ae}. Figure 10 illustrates the oversampling phenomena of samplers facing into the wind and sampling at $u/u_o < 1$. According to Fig. 10, c/c_o for the 37-mm IL cassette increases above 11-μm D_{ae}, but the theory for thin-wall samplers predicts it should turn slightly downward because at 2 m/s u/u_o is > 1. This experimental result conflicts with thin-wall theory, but cannot be considered erroneous because no accepted theory for thick-wall samplers exists.

$\alpha \neq 0°$

Results from sampling tests at 90 and 180° angles of incidence (α) are listed in Table IV and illustrated as a function of STK in Figs. 11 and 12. Below STK = 0.1 all cassettes appear to have a fractional collection efficiency close to 1; however, as STK increases all cassettes exhibit a decrease in efficiency. The decrease is least for the 37-mm OF cassette both at $\alpha = 90°$ and $\alpha = 180°$. This phenomenon may occur because the large inlet diameter of the OF cassette produces eddies (vortices) which spill from the inlet lip to bring particles under the influence of the sampling airflow.

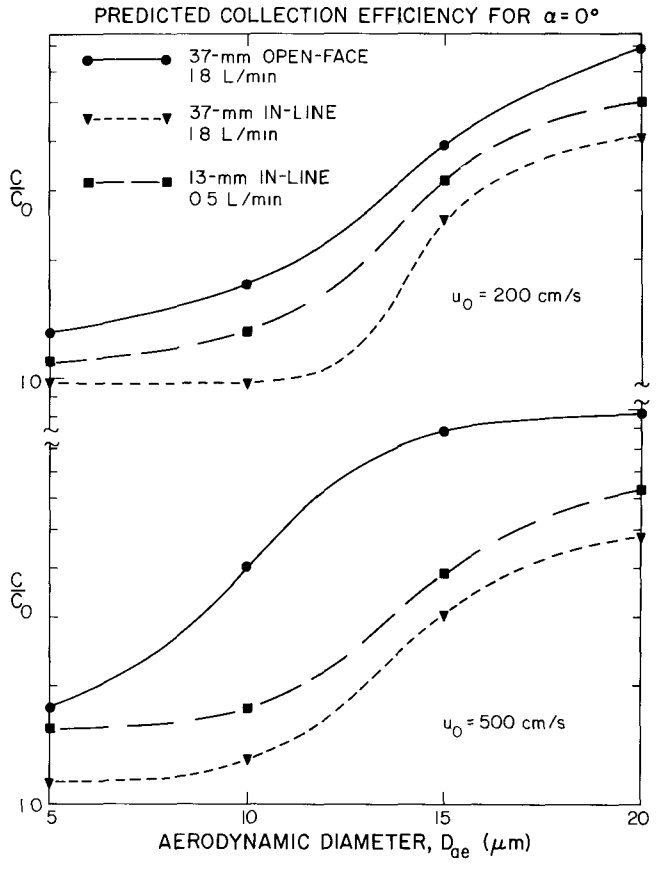

Fig. 10.
Collection efficiency (c/c_o) predicted by Eqs. (10) and (11) for $\alpha = 0°$.

The same analytical approach used for $\alpha = 0°$ (relating c/c_o to A_1) was tried for sampling results from $\alpha = 90$ and 180° tests even though no theoretical justification exists for a correlation between A_1 and c/c_o at $\alpha \neq 0°$. Surprisingly, c/c_o correlated with A_1 better for $\alpha = 90$ and 180° sampling than it did for $\alpha = 0°$ sampling. However, no spheres larger than 11.2-μm D_{ae} (Table IV) were used in the 90 and 180° sampling.

Results from sampling at an angle to the wind are correlated as $c/c_o/A_1$ vs A_1 from Table IV for 90° samples in Fig. 13 and for 180° samples in Fig. 14. Although the results do not fall on a common line as they do for $\alpha = 0°$ samples (Fig. 9, D_{ae} <12-μm data), the data for each particular sampler cassette exhibit good correlation both at $\alpha = 90°$ and $\alpha = 180°$. The data for the 37-mm in-line and 13-mm in-line cassettes nearly coincide, probably because the inlet inside diameters of these two cassettes are almost identical, whereas the 37-mm open-face cassette inlet is much larger. The 37-mm OF cassette is least sensitive to incidence angle. For the OF cassette the curves for 90 and 180° (Figs. 13 and 14) are only slightly steeper than that for 0° (Fig. 9, <12-μm D_{ae}).

Regression analysis of the results for $\alpha = 90$ and 180° orientation tests produced the functions listed in Table V. All of the results follow a power function of A_1 with a minimum correlation coefficient, $r = 0.84$. Equations from Table V were used to calculate the curves shown in Fig. 15 for U_o = 200 cm/s. These empirical, predictive curves indicate that collection efficiency is sensitive to angle of incidence of the wind, more so for the 13-mm IL cassette than for the others. The minimum c/c_o for the 13-mm IL cassette occurs at 90° incidence angle for all particle sizes,

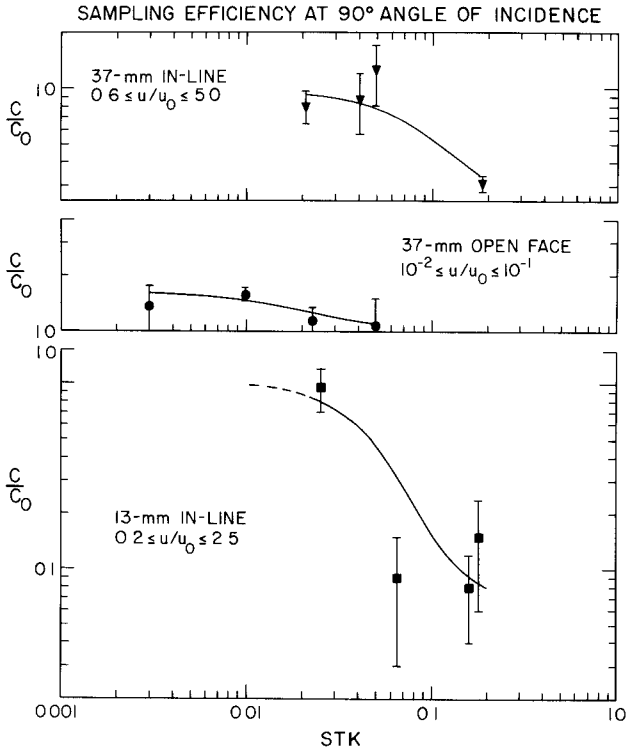

Fig. 11.
Measured collection efficiency (c/c_o) as a function of STK in three wind conditions and two sampling flow rates at α = 90°.

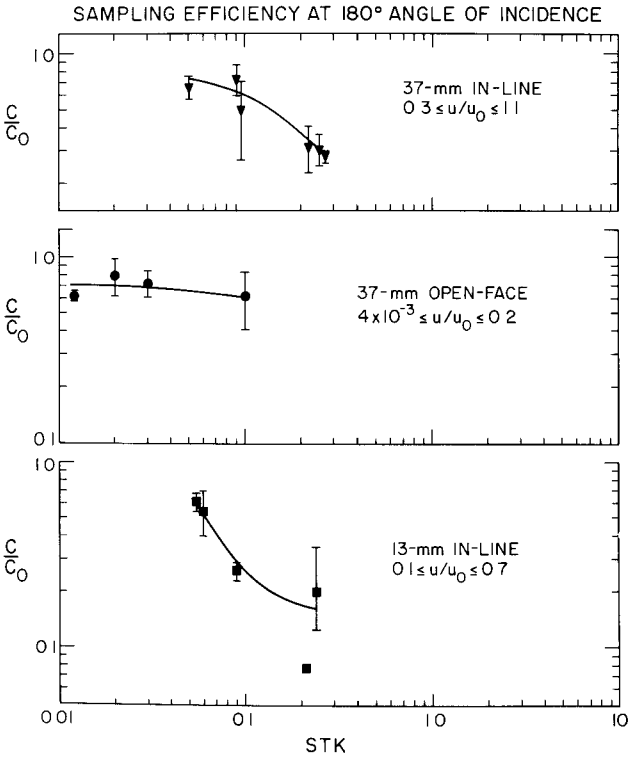

Fig. 12.
Measured collection efficiency (c/c_o) as a function of STK in three wind conditions and two sampling flow rates at α = 180°.

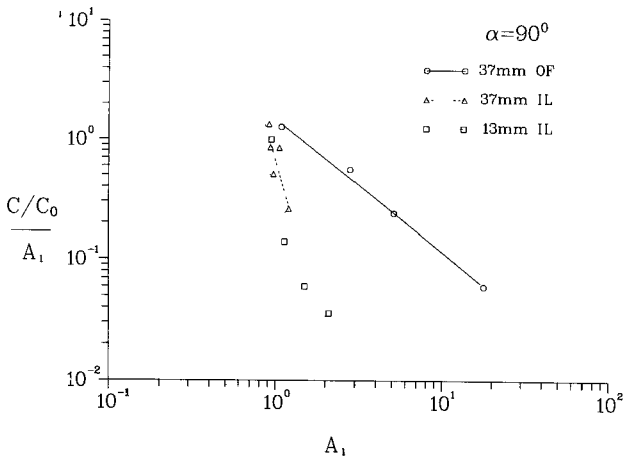

Fig. 13.
Measured collection efficiency (c/c_o) normalized to A_1, plotted as a function of A_1 for all sampling conditions at α = 90°.

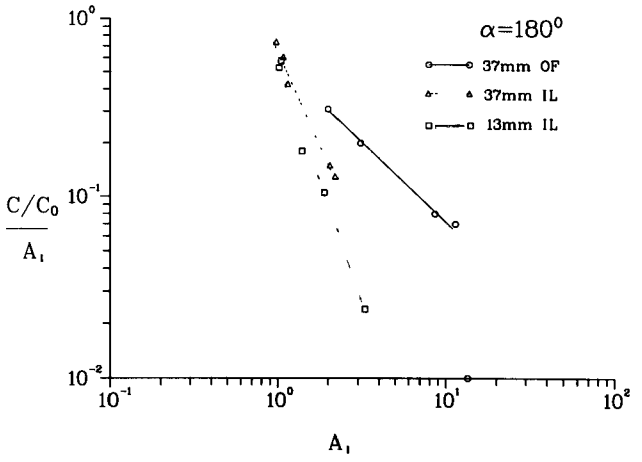

Fig. 14.
Measured collection efficiency (c/c_o) normalized to A_1, plotted as a function of A_1 for all sampling conditions at α = 180°.

TABLE IV

SAMPLING RESULTS FOR $\alpha = 90^\circ$ and 180°

Sampling Conditions and Cassettes	u_o	u/u_o	D_{ae}	STK	c/c_o [a]	A_i	$c/c_o/A_i$
STANDARD FLOW							
$\alpha = 90^\circ$							
1L [b]	5.1	0.62	3.7	0.041	(1) 0.89	1.05	0.85
	5.1	0.59	7.7	0.19	(4) 0.31 ± 0.03 (9)	1.20	0.26
OF	3.9	0.01	5.0	0.01	(3) 1.58 ± 0.13 (8)	2.8	0.56
	3.9	0.01	7.5	0.023	(4) 1.13 ± 0.21 (18)	5.1	0.22
	3.9	5.0×10^{-3}	11.2	0.05	(2) 1.08	17.8	0.06
13-mm	3.9	0.18	4.7	0.065	(4) 0.09 ± 0.06 (66)	1.49	0.06
	3.9	0.18	7.2	0.16	(2) 0.08	2.14	0.04
1L	1.9	4.7	4.7	0.009	(3) 0.50 ± 0.02 (5)	0.97	0.52
	1.9	4.7	8.0	0.021	(4) 0.80 ± 0.16 (20)	0.93	0.86
	0.5	2.5	11.2	0.05	(2) 1.25	0.91	1.38
OF	0.5	0.08	7.5	0.003	(2) 1.37	1.08	1.27
13-mm	0.5	2.5	7.8	0.025	(2) 0.95	0.95	1.00
	1.8	0.73	11.2	0.18	(2) 0.15	1.11	0.14
$\alpha = 180^\circ$							
1L	5.1	0.25	7.8	0.25	(3) 0.31 ± 0.06 (21)	2.05	0.15
OF	5.2	8.0×10^{-3}	7.8	0.030	(3) 0.72 ± 0.12 (17)	8.6	0.08
13-mm	5.1	0.12	7.7	0.21	(1) 0.08	3.3	0.02
1L	1.9	1.14	7.8	0.09	(3) 0.73 ± 0.10 (14)	0.98	0.74
OF	1.9	0.21	7.8	0.012	(3) 0.62 ± 0.04 (6)	2.0	0.31
13-mm	1.9	0.29	7.8	0.09	(3) 0.26 ± 0.03 (11)	1.40	0.18
1/2 STANDARD FLOW							
$\alpha = 180^\circ$							
1L	5.1	0.21	7.3	0.25	(3) 0.28 ± 0.02 (6)	2.2	0.13
OF	5.1	3.5×10^{-3}	6.2	0.02	(6) 0.79 ± 0.18 (22)	11.4	0.07
	5.1	3.7×10^{-3}	7.2	0.027	(3) 0.12 ± 0.03 (25)	13.5	0.01
13-mm	5.1	0.25	7.3	0.24	(3) 0.20 ± 0.15 (78)	1.93	0.10
1L (WT)	5.0	0.24	7.6	0.22	(4) 0.32 ± 0.09 (28)	2.04	0.15
1L	1.9	0.59	6.2	0.05	(6) 0.66 ± 0.09 (13)	1.08	0.61
	1.9	0.58	7.2	0.09	(3) 0.49 ± 0.22 (45)	1.14	0.43
OF	1.9	0.01	7.3	0.01	(3) 0.62 ± 0.21 (35)	3.1	0.20
13-mm	1.9	0.68	6.2	0.06	(6) 0.61 ± 0.07 (12)	1.06	0.58
	1.9	0.68	7.2	0.06	(3) 0.54 ± 0.14 (26)	1.02	0.53

[a] c/c_o is in the format: (No. of samples) mean ± std dev (COV).
[b] Cassettes are: IK, 37-mm ISOKINETIC; IL, 37-mm IN-LINE; OF, 37-mm OPEN-FACE; 13-mm, 13-mm IN-LINE; (WT), tested in wind tunnel.

TABLE V

SAMPLING RESULTS FOR $\alpha = 90^\circ$, 180°

Sampler; Conditions	Function	Range	No. of Samples	Correlation Coefficient r
IL; $\alpha = 90^\circ$, std flow	$c/c_o/A_i = 0.7\ A_i^{-4.75}$	$0.9 \leq A_i \leq 1.2$	5	0.84
OF; $\alpha = 90^\circ$, std flow	$c/c_o/A_i = 1.5\ A_i^{-1.11}$	$1.1 \leq A_i \leq 18$	4	0.99
13-mm; $\alpha = 90^\circ$, std flow	$c/c_o/A_i = 0.4\ A_i^{-3.52}$	$0.9 \leq A_i \leq 2.2$	4	0.88
IL; $\alpha = 180^\circ$, std and 1/2 std	$c/c_o/A_i = 0.7\ A_i^{-2.09}$	$1.0 \leq A_i \leq 2.2$	6	0.99
OF; $\alpha = 180^\circ$, std and 1/2 std	$c/c_o/A_i = 0.9\ A_i^{-1.36}$	$2.0 \leq A_i \leq 12$	5	0.87
13-mm; $\alpha = 180^\circ$, std and 1/2 std	$c/c_o/A_i = 0.6\ A_i^{-2.67}$	$1.0\ A_i \leq 3.3$	5	0.99

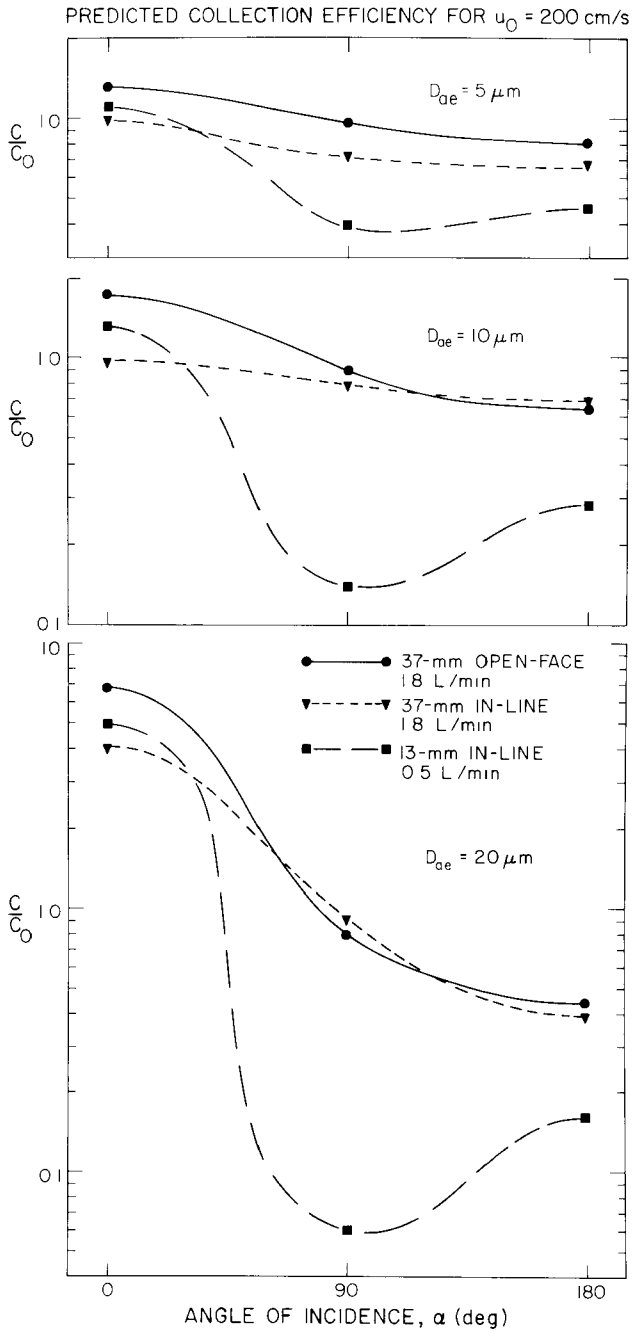

Fig. 15.
Collection efficiency (c/c_o) predicted by Eqs. (10), (11), and those in Table IV for standard flow rate and u_o = 200 cm/s.

whereas, for the 37-mm OF and IL cassettes minimum c/c_o occurs at $\alpha = 180°$. Raynor[8] found that an open-face type, thick-wall holder ($D/l = 1.7$) also exhibited minimum collection efficiency at $\alpha = 90°$. The predicted results for 20-μm D_{ae} particles in Fig. 13 are extrapolations since no experiments at $\alpha = 90$ and 180° were conducted with particles larger than 11-μm D_{ae}.

RAC AND WT COMPARISON

As stated earlier, limited tests were made in a small wind tunnel to determine the similarity in performance of the cassettes in the WT and RAC. Only two cassettes, a 37-mm IL type and an identical cassette fitted with an isokinetic probe, were tested and compared in the WT. Comparison with an isokinetic probe was necessary because no stationary reference samples could be obtained in the WT, as they were in the RAC. A velocity of 5 m/s and challenge aerosols of 4- and 7-μm D_{ae} were used in the WT tests.

Results from WT runs are designated in Tables III and IV with the notation WT under the first column. No stationary reference samples were obtainable in WT runs; consequently, the WT results cannot be compared directly to results in the RAC. However, since identical IK samplers were used in both chambers, the results can be compared from the listed c/c_o and A_i (Table III) for 7.2- and 7.4-μm D_{ae} for the IK and IL samplers. Using C_{IL} and C_{IK} to denote concentrations obtained from the 37-mm in-line and isokinetic samplers, respectively, the development is:

$$C_{IK}/C_o = 0.97 \text{ in RAC (Table III, row 2, } c/c_o) \tag{12}$$

$$\text{and } C_{IL} = 1.25 \text{ in RAC (Table III, row 5, } c/c_o) \tag{13}$$

$$\text{then } C_o = C_{IK}/0.97 \tag{14}$$

$$\text{and } C_{IL}/C_o = C_{IL}/(C_{IK}/0.97) = 1.25 \text{ in RAC ,} \tag{15}$$

$$\therefore\ C_{IL}/C_{IK} = 1.29 \text{ in RAC .} \tag{16}$$

$$\text{Also } C_{IL}/C_{IK} = 1.08 \text{ in the WT (Table III, 5 m/s, last row, } c/c_o) \text{ .} \tag{17}$$

But these concentration ratios are for slightly different A_i and must be normalized to the same A_i (equivalent conditions). Thus from (16) and A_i in Table III (rows 5 and 14):

$$C_{IL}/C_{IK}\ A_i^{-1} = 1.29/1.41 = 0.91 \text{ in the RAC ,} \tag{18}$$

$$\text{and } C_{IL}/C_{IK} \cdot A^{-1} = 1.08/1.35 = 0.80 \text{ in the WT .} \tag{19}$$

Therefore C_{IL}/C_{IK} in the RAC, and (C_{IL}/C_{IK}) in WT are (0.91-0.80)/0.80 = 13.7% different for equivalent A_i. The minimum error in the experimental data may be estimated from the coefficient of variation (CoV) from Table III:

$$\text{Error} = [(\text{CoV of IK})^2 + (\text{CoV of IL})^2]^{1/2} = [(0.17)^2 + (0.07)^2]^{1/2} = 0.18 \text{ or } 18\%$$

This indicates that the difference between sampling efficiency determined in the two chambers (13.7%) is less than the experimental error in measurement. Thus the RAC and WT give equivalent sampling efficiencies for the test cassettes.

Throughout the cassette testing the wall losses (deposition) of a fraction of the cassettes were determined. Losses due to deposition were generally high and variable, but proportional to the challenge aerosol particle size. The losses at $U_o = 5$ m/s were slightly greater than at $U_o < 5$ m/s but this difference was not quantitated. The 37-mm IL cassette with isokinetic probe exhibited the largest losses at $\alpha = 0°$ (Table VI), probably due to the small diameter and long entrance length of the probe. At 90 and 180° insufficient numbers of samples were measured to serve to define losses at sizes other than 8-μm D_{ae}, but at $\alpha = 180°$, these particles produced the greatest wall losses measured. In all angles of incidence, average losses (for a particular cassette) were used to estimate losses in collection efficiency tests for which no loss data were obtained. As noted previously, data in Tables II through IV (and Figs. 6-13) have been corrected for actual or estimated wall losses. The average loss for each cassette is shown in Table VI, with number of samples in parentheses before the mean value, and CoV in parentheses after the standard deviation. The large CoVs indicate the variability of the wall losses.

TABLE VI

WALL DEPOSITION LOSSES (%) IN TEST CASSETTES

		Nominal Particle Diameter, D_{ae} (μm)			
Cassette	α	4	6	8	21
IK	0°	(2)15[a]	(10)19±12(60)	(17)22±11(49)	(9)47±26(56)
37-mm IL	0°	(3)8±6(76)	(4)9±10(116)	(13)17±19(110)	(10)19±20(102)
37-mm OF	0°	---	(6)8±4(53)	(10)11±10(90)	(9)34±17(50)
13-mm IL	0°	---	(2)15	(3)13±9(71)	(7)36±22(59)
25-mm IL[b]	0°	---	---	(3)6±3(47)	(12)14±8(55)
37-mm IL	90°	(2)5	(2)4	(4)5±2(40)	---
37-mm OF	90°	(2)4	(2)10	(6)12±6(49)	---
13-mm IL	90°	(1)46	(1)21	(2)6	---
37-mm IL	180°	---	---	(6)47±13(28)	---
37-mm OF	180°	---	---	(3)59±20(33)	---
13-mm IL	180°	---	---	(3)45±17(37)	---

[a] Wall losses are shown in the format: (Number of samples) mean wall loss ± standard deviation (CoV). All in %, except number of samples.

[b] 25-mm IL cassettes were used as stationary reference samplers, collecting at 5.0 L/min flow rate.

SUMMARY OF RESULTS

Based on the empirical functions found to correlate test results with Eqs. (8) and (9), it is possible to predict the performance of the cassettes under various conditions. The predicted performance was shown in detail in Figs. 10 and 15. A summary of predicted performance for various sampling conditions is listed in Table VII. The conditions of wind, angle of incidence, and D_{ae} are listed for which each cassette can be expected to provide a sampled concentration within 20% of the true or reference concentration. Thus, for calm conditions all three cassette samplers can be expected to provide a representative sample for particles with D_{ae} to at least 15 μm. On the other hand, none of the samplers provide a valid sample if the wind is 200 cm/s or greater from behind the cassette inlet, with the exception that the OF cassette will provide a valid sample of particles not exceeding 5-μm D_{ae}. The absence of entries for u_o = 500 cm/s and α = 90 or 180° indicates that none of the cassettes sample efficiently under these conditions for any particle size tested. The results from Table VII as well as Figs. 10 and 15 are valid only for cassette samples for which the wall losses have been determined and included in the determination of concentration.

CONCLUSION

Aerosol concentrations determined by test samplers facing into the wind were generally within 20% of those determined by reference sampler for aerosols with D_{ae} <5 μm after correction for wall losses. In calm wind conditions the cassettes were within 20% for $D_{ae} \leq 15$ μm. However, as particle size was increased, sampling efficiencies of the test cassettes differed increasingly from theoretically calculated efficiences at both calm and windy conditions. This departure from Belyaev and Levin's theory for thin-wall samplers was consistent even though the reason for the disparity is unknown. In spite of the disparity, Belyaev and Levin's theory and Davies' modification for calm sampling can be used to develop predictive equations for the test cassettes sampling at angles of incidence of 0, 90, and 180°. Predictive equations can be based upon the "thin-wall" sampler theory because it contains two of the same parameters that determine thick-wall sampler performance, namely u/u_o and STK.

Using criteria described in the summary some specific conclusions concerning the cassettes may be stated.

- **In calm winds, sampling error is <20% for all cassettes for $D_{ae} \leq 15$ μm.**
- **The 37-mm OPEN-FACE cassette exhibits large error when sampling into a wind (α = 0°).**
- **The 37-mm IN-LINE cassette exhibits <20% error for $D_{ae} \leq 9$ μm for all test conditions except α = 180°.**
- **The 13-mm IN-LINE cassette exhibits ≤20% error for $D_{ae} \leq 25$ μm in calm winds, but when sampling against winds, particularly at α = 90 and 180°, its error exceeds 30%.**

TABLE VII

SUMMARY OF CONDITIONS FOR WHICH THE CASSETTES MEASURE WITHIN ±20 PERCENT OF TRUE CONCENTRATION

Conditions		Size range, aerodynamic diam, D_{ae} (μm)		
Wind cm/s	α degrees	37-mm OPEN-FACE	37-mm IN-LINE	13-mm IN-LINE
Calm	—	≤15	≤15	≤25
200	0	none	≤12	≤ 8
500	0	none	≤ 9	none
200	90	≤20	≤20	none
200	180	≤ 5	none	none

The 37-mm IL cassette apparently provides the best sampling efficiency for most conditions in spite of its complex inlet geometry. Finally, it must be cautioned that wall losses are significant in all the cassettes for $D_{ae} > 6$ μm and must be accounted for in use.

ACKNOWLEDGMENT

Mrs. Bonnie Isom, Group H-5, Los Alamos Scientific Laboratory, performed the SEM photomicrography required for this study.

REFERENCES

1. G. A. Sehmel, "Complexities of Particle Deposition and Reentrainment in Turbulent Pipe Flow," J. Aerosol Sci. **2**, 63-72 (1971).

2. S. P. Belyaev and L. M. Levin, "Investigation of Aerosol Aspiration by Photographing Particle Tracks Under Flash Illumination," J. Aerosol Sci. **3**, 127-140 (1972).

3. S. P. Belyaev and L. M. Levin, "Techniques for Collection of Representative Aerosol Samples," J. Aerosol Sci. **5**, 325-338 (1974).

4. S. Badzioch, "Collection of Gas-Borne Dust Particles By Means of an Aspirated Sampling Nozzle," Brit. J. Appl. Phys. **10**, 26-32 (1959).

5. V. M. Voloshchuk and L. M. Levin, "A Study of Aerosol Aspiration," Trans. Inst. Exp. Met., No. 1, 84-105 (1969).

6. C. N. Davies, personal communication, 1980.

7. M. D. Durham and D. A. Lundgren, "Evaluation of Aerosol Aspiration Efficiency as a Function of Stokes Number, Velocity Ratio and Nozzle Angle," J. Aerosol Sci., **11**, 179-188 (1980).

8. G. S. Raynor, "Variation in Entrance Efficiency of a Filter Sampler with Air Speed, Flow Rate, Angle and Particle Size," Am. Ind. Hyg. Assoc. J. **31**, 294-304 (1970).

9. N. Rajendran, "Theoretical Investigation of Inlet Characteristics for Personal Aerosol Samplers," IIT Research Institute report, 128 pp. (1979).

10. N. A. Fuchs, "Sampling of Aerosols," Atm. Env. **9**, 697-707 (1975).

11. W. K. Lautner and G. T. Fisher, "Ragweed Pollen Generation and Sampling Methods for Filtration Studies," Am. Ind. Hyg. J. **36**, 303-310 (1975).

☆U S. GOVERNMENT PRINTING OFFICE: 1980—777-022/220

Printed in the United States of America
Available from
National Technical Information Service
US Department of Commerce
5285 Port Royal Road
Springfield, VA 22161

Microfiche $3.50 (A01)

Page Range	Domestic Price	NTIS Price Code	Page Range	Domestic Price	NTIS Price Code	Page Range	Domestic Price	NTIS Price Code	Page Range	Domestic Price	NTIS Price Code
001-025	$ 5.00	A02	151-175	$11.00	A08	301-325	$17.00	A14	451-475	$23.00	A20
026-050	6.00	A03	176-200	12.00	A09	326-350	18.00	A15	476-500	24.00	A21
051-075	7.00	A04	201-225	13.00	A10	351-375	19.00	A16	501-525	25.00	A22
076-100	8.00	A05	226-250	14.00	A11	376-400	20.00	A17	526-550	26.00	A23
101-125	9.00	A06	251-275	15.00	A12	401-425	21.00	A18	551-575	27.00	A24
126-150	10.00	A07	276-300	16.00	A13	426-450	22.00	A19	576-600	28.00	A25
									601-up	†	A99

†Add $1.00 for each additional 25-page increment or portion thereof from 601 pages up.